Available online at www.sciencedirect.com
SCIENCE DIRECT®
Polymer 45 (2004) 1485–1493
polymer
www.elsevier.com/locate/polymer

A new route for organic–inorganic hybrid material synthesis through reactive processing without solvent

V. Bounor-Legaré, C. Angelloz, P. Blanc, P. Cassagnau, A. Michel*

Laboratoire des Matériaux Polymères et des Biomatériaux, Bât. ISTIL, Université Claude Bernard LYON 1, UMR CNRS 5627 15, Boulevard Latarjet, 69622 Villeurbanne cedex, France

Received 31 July 2003; received in revised form 26 November 2003; accepted 2 December 2003

Abstract

A new route to elaborate organic–inorganic hybrid materials is presented. It is based upon two successive steps, the former is the crosslinking of polymer which contains pendant ester groups such as poly(ethylene–co-vinyl acetate) (EVA) through ester–alkoxysilane interchange reaction in molten state in the presence of dibutyltin oxide as catalyst. The latter is the hydrolysis–condensation reactions of available alkoxysilane groups in the polymer network leading to the silica network co-grafted onto the organic network. More particularly the hydrolysis–condensation reactions in solid state leading to the silica network grafted and confined in the organic network are addressed in the present work. The progress of the hydrolysis–condensation reactions was investigated by gas chromatography, FT-IR spectroscopy, ^{29}Si solid NMR, volume swelling degree at equilibrium and dynamic mechanical analysis. Two side reactions have been evidenced leading to alcohol groups grafted onto EVA. The silanols and these alcohol groups can participate to hydrogen bonds between ester and silica domains. The organic–inorganic hybrids elaborated according to this new chemical route exhibit improved mechanical and thermomechanical properties with respect to the EVA while having an elastomeric behavior with respect to the nanocomposite synthesized by in situ polymerization of tetraethoxysilane.

Keywords: Organic–inorganic hybrids; Ester–alkoxysilane exchange reaction

1. Introduction

From the literature data, two types of organic–inorganic hybrid materials produced by sol–gel process are considered [1]. In the first type, there is no covalent bonding between organic and inorganic phases but mainly hydrogen bonding between the two phases. These organic–inorganic materials are elaborated by mixing an organic polymer with a metal alkoxide such as a tetraalkoxysilane in the presence of a solvent [2–3]. The sol–gel process based upon hydrolysis–condensation reactions of the metal alkoxide leads to an inorganic network that causes the precipitation and dispersion of inorganic fillers throughout the polymer matrix [4–8]. The word of nanocomposites seems to be more appropriate for such materials because they behave as thermoplastics with inorganic fillers. The molecular motions of the organic polymer matrix are not restricted. The second class of organic–inorganic hybrid materials implies the existence of covalent bonds between polymer matrix and inorganic phase. Then the molecular motions of the organic polymers being restricted, the thermomechanical properties are improved with respect to nanofillers only dispersed in organic polymers. Two main routes are described in the literature to elaborate this class of hybrids through the sol–gel process including hydrolysis–condensation reactions of metal alkoxides. The first one consists in making react metal alkoxides with either reactive end-capped organic polymers or oligomers or copolymers containing pendant metal alkoxide groups in solution [3,9,10]. The second one consists in doing to react monomers containing metal trialkoxide groups in solution [11–14] through hydrolysis–condensation reactions and then to initiate polymerization of monomer grafted onto inorganic phase. In all the papers concerning the elaboration of either nanocomposites or organic–inorganic hybrids, there is always the use of a solvent, which limits the application to coatings of glass, metal and polymer substrata. Few others methods were proposed to elaborate either nanocomposites or organic–inorganic hybrids for example in

* Corresponding author. Tel.: +33-472432701; fax: +33-472-431249.
E-mail address: a-michel@univ-lyon1.fr (A. Michel).

0032-3861/$ - see front matter © 2003 Elsevier Ltd. All rights reserved.
doi:10.1016/j.polymer.2003.12.027

swelling elastomer with a tetraalkoxysilane solution [15–17]. Recently, a modification of a polyethylene-octene elastomer through an in situ sol–gel process was carried out by incorporation of a solution containing a silica precursor, water and a catalyst [18] in the molten polymer.

This paper deals with an original route to obtain organic–inorganic hybrid materials in molten state without the presence of solvent and that can be integrated into processing operations of thermoplastic polymers such as extrusion. Then it offers the possibility to tailor articles made of organic–inorganic hybrids in bulk. This route is based upon two successive steps, the crosslinking of ethylene-co-vinyl acetate copolymers (EVA) through the ester–alkoxysilane interchange [19] reaction in the presence of a tetraalkoxysilane and the hydrolysis–condensation reactions of alkoxysilane groups trapped either in the crosslinking bridges or free but confined in the polymer network. The hydrolysis–condensation reactions are carried out according to the Sioplast [20] process on the sample after shaping process.

2. Experimental part

2.1. Materials and reagents

EVA copolymer was supplied by Elf-AtoFina (Evatane® 2803). Its amount of vinyl acetate units (VA) is 28% by weight [21,22], which corresponds to a molar composition of 10.6% of VA units. It presents a melting point around 75 °C. Number average molecular weight ($M_n = 19,000$ g mol^{-1}) and weight average molecular weight ($M_w = 53,500$ g mol^{-1}) were measured by size exclusion chromatography in trichlorobenzene at 135 °C using a linear polyethylene NBS calibration. The microstructure of this copolymer was determined by ^{13}C NMR. 95% of VA units are isolated and 5% are in diads and triads. Tetrapropoxysilane (TPOS) and dibutyltin oxide (DBTO) were obtained, respectively, from Roth Sochiel and Aldrich and used without further purification. HCl 1 N for the hydrolysis–condensation reactions is also supplied by Aldrich.

2.2. Preparation of hybrid material

The alkoxysilane concentration is defined through the molar ratio between the number of vinyl acetate units (VA) and the number of alkoxide groups (OR) from TPOS. The concentration of DBTO as precursor of distannoxane catalyst [22–25] was fixed to 1 phr (gram per hundred grams of EVA). EVA copolymer, TPOS and DBTO were mixed during 3 min at 110 °C in an internal mixer equipping a Haake Rheomixer. Using these processing conditions, there is no crosslinking of the EVA. The crosslinking reaction was then carried out at 150 °C during 45 min between the plates of a heating press. After crosslinking, the hydrolysis–condensation reactions of the samples were carried out on sheets of 1 mm thickness embedded in acidic water (HCl 1 N) at 80 °C according to the Sioplast process [20].

References, without DBTO and so without crosslinking reaction, were also prepared in the same conditions as above in order to study the influence of the organic network on the hydrolysis–condensation reactions kinetic on the overall conversion.

2.3. Characterization of hybrid material

The progress of the hydrolysis–condensation reactions was followed by gas chromatography analysis of the propanol released in water with the help of a capillary column filled with polyethylene glycol-terephthalic acid as stationary phase (length = 15 m, diameter = 0.53 mm, phase thickness = 1.5 mm). Temperature profile is 1 min at 50 °C and heating rate of 70 °C min^{-1} up to 200 °C; flame ionization detector is used with an oxygen output of 30 ml min^{-1} and hydrogen output of 43 ml min^{-1}. Carrier gas was nitrogen (from 0.8 bar at 80 °C to 1.3 bar at 200 °C). In these analytical conditions, the retention time of the *n*-propanol is 0.55 min and the acetic acid as side product has been detected at the retention time of 2.14 min.

The calibration constant (signal/concentration) is 2.21×10^8 for the *n*-propanol.

Infrared spectra were obtained with a Nicolet FTIR spectrometer 20SX on KBr pellets after cryogrinding of crosslinked materials in liquid nitrogen.

^{29}Si CP-MAS NMR spectra were obtained using a BRUKER AC200 apparatus equipped with a solid accessory, working at 39.76 MHz. The samples were spun at 5 kHz. Pulse interval times were 2 s. The contact time was 7 ms. All the chemical shifts were referenced to tetramethylsilane. Typically, around 100–200 mg of powder of each sample obtained by cryogrinding in liquid nitrogen were used.

The crosslinking density was assessed from the volume swelling degree determination at equilibrium [22]. Samples (50–80 mg) were embedded in hot toluene at 80 °C during 48 h so that the swelling equilibrium is reached.

The polymer volume fraction at swelling equilibrium ν_2, was calculated as follows:

$$\nu_2 = \frac{1}{1 + \left(\frac{m_1}{m_2}\right)\frac{\rho_2}{\rho_1}}$$

Where m_1 and m_2 are, respectively, the mass of solvent swelling the sample and the mass of dried crosslinked sample and $\rho_2 = 0.95$ and $\rho_1 = 0.895$ are, respectively, the polymer and solvent densities (g cm^{-3}).

A review of various models that predict the extent of swelling that the network undergoes when placed in good solvent and the relationships with the elastic modulus was

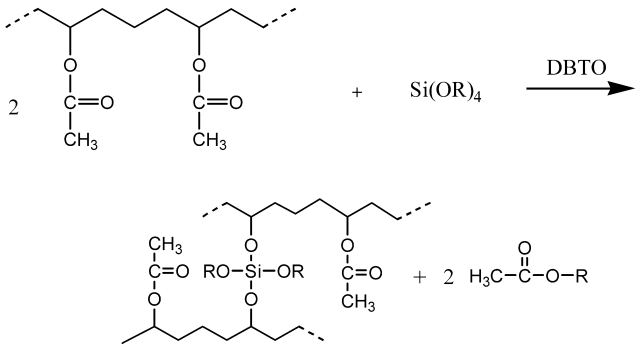

Fig. 1. Reaction scheme of the EVA crosslinking through ester–alkoxysilane interchange reaction (R = propyl).

made, as for example, by Patel et al. [26]. In particular, they found that the Flory–Rhener model coupled with the phantom network assumption gives a relation between the swelling results and the number of elastic strands ν:

$$-\left[\frac{Ln(1-\nu_2)+\nu_2+\chi\nu_2^2}{V_1\nu_2^{1/3}}\right]=\nu$$

Where χ is the polymer/solvent interaction parameter, V_1 the molar volume of solvent and ν_2 is the polymer volume fraction at equilibrium swelling. In a previous study [22], we found that χ parameter is ν_2 dependent for EVA/toluene system as:

$$\chi = 0.059 + 0.345\nu_2$$

Furthermore, assuming a perfect network, the relationship between the number ν of elastic strands and crosslinking density μ (mol ml^{-1}) is:

$$\mu = 2\nu/f$$

In our case with a functionality of crosslinking bridge equal to 4: $\mu = \nu/2$.

Dynamic mechanical properties were obtained with a Rheometrics mechanical spectrometer (RMS 800) using the rectangular torsion method between −150 and 200 °C and with a torsion rate of 1 rad s^{-1}. The strain was manually fitted from 0.05% at low temperature (below T_g) to approximately 1% at high temperature in order to remain in the domain of linear viscosity.

The stress–strain curves were obtained by using an Instron 1175 at room temperature. H3 type dumbbell shaped samples were used. The strain speed was 50 mm min^{-1}.

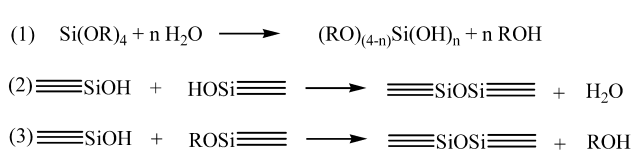

Fig. 2. Reaction scheme of alkoxysilane showing the hydrolysis (1) and the condensation reactions (2) and (3).

3. Results and discussion

3.1. Nature of the chemical reactions

In a first step, as previously shown [19], the EVA is crosslinked at 150 °C through the interchange reaction ester-tetrapropoxysilane according to the scheme in Fig. 1 with R = propyl.

From the previous kinetic and rheological data [19], we showed that in average two alkoxide groups of one TPOS molecule are involved in this exchange reaction. In the present case, after 45 min of curing, the assessment of propyl acetate by gas chromatography showed that only 4 and 10% of acetate groups have reacted, respectively, for molar ratio VA/OR = 1 and 0.5. So, for VA/OR = 1 and 0.5, respectively, 8 and 10% of TPOS are engaged in the crosslinking bridges. In consequence, respectively, 92% and 90% of the TPOS is free and dispersed in the EVA network. In a second step, the hydrolysis–condensation reactions of alkoxide groups are carried out on crosslinked EVA at 80 °C in acidic water and leads to the silica network according to the scheme in Fig. 2.

The condensation reactions (2) and (3) between silanol groups inserted in the crosslinking bridges and free silanol groups in the EVA network leads to connectivity between the organic phase and the inorganic network formed in situ according to the scheme in Fig. 3. In this Fig. 3, the different species Q^1, Q^2, Q^3 and Q^4 which are formed during tetraalkoxysilane polymerization are identified by solid ^{29}Si NMR [27,28]. These results will be discussed later.

3.2. Evolution of hydrolysis–condensation reactions (1) and (3) by gas chromatography

The propanol released in acidic water during hydrolysis and condensation reactions (1) and (3) of remaining alkoxysilane groups was assessed by gas chromatography analysis (Fig. 4).

Without crosslinking, the hydrolysis–condensation reactions of TPOS dispersed in EVA copolymer (VA/OR = 0.5) showed that about 80% of the alkoxysilanes have reacted in less than 1 h and that the conversion reaches a plateau value of about 85% after 50 h. In the case of crosslinked EVA sample, the speed of propanol formation is slowed down and the conversion tends towards a plateau of about 70% for VA/OR = 0.5 and of about 60% for VA/OR = 1 after 50 h of hydrolysis. These results show that the hydrolysis–condensation reactions of tetrapropoxysilane is not complete in molten EVA matrix at 80 °C and that the phenomenon is emphasized by the first step of crosslinking, suggesting that the accessibility of the SiOR groups confined in the polymer network is reduced.

Furthermore, deeper analysis of the chromatogram showed the appearance of acetic acid peak due to a side reaction during hydrolysis. To explain the origin of the acetic acid further experiments were carried out in the same

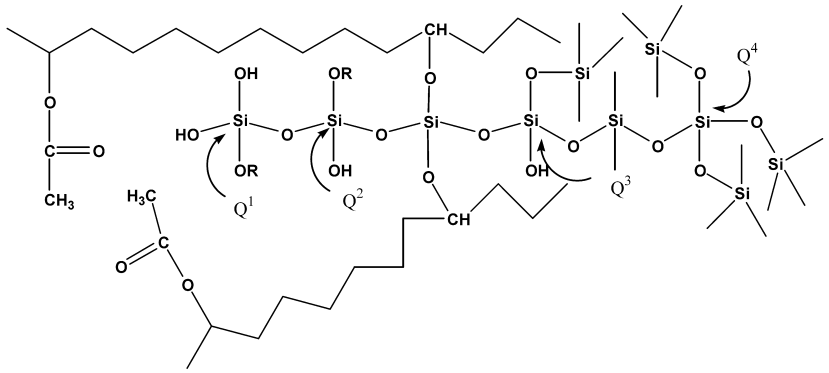

Fig. 3. Reaction scheme of silica network growing and its grafting on EVA network.

conditions of hydrolysis after a curing time of 45 min at 150 °C. In these experiments, the qualitative determination of acetic acid was made by high performance liquid chromatography (HPLC) analysis of the hydrolytic medium.

EVA alone and EVA/TPOS blend (VA/OR = 1) do not exhibit the formation of acetic acid during hydrolysis. On the other hand for the blend EVA/DBTO (1 phr) there is appearance of acetic acid during hydrolysis.

This result suggests that the acetic acid formation during hydrolysis is due to the hydrolysis of acetoxy-alkoxy distannoxane as product of reaction of DBTO with acetate groups [23,24] of the EVA. This assumption was confirmed by the hydrolysis of acetoxy-octanoxy distannoxane, as model compound of distannoxane grafted onto EVA backbone by reaction of DBTO with acetate groups.

So the acetoxy-alkoxydistannoxane is not only the catalyst of ester–alkoxysilane interchange reaction but it is also at the origin of a side reaction leading to pendant alcohol groups along the EVA chains according to the chemical scheme in Fig. 5.

3.3. Evolution of crosslinking density (μ) during hydrolysis–condensation reactions

During hydrolysis–condensation reactions, the connectivity between the EVA network and the growing silica domains according the chemical scheme (Fig. 3) is developed through Si–O–C bonds of crosslinking bridges arising from crosslinking step. These Si–O–C bonds can be also sensitive to hydrolysis and lead to a decrease of the connecting bonds between organic and inorganic phases and formation of pendant alcohol groups according to the chemical scheme (Fig. 6). The importance of this side reaction was approached through the evolution of the crosslinking density of EVA during the step of hydrolysis–condensation determined by the assessment of the volume swelling rate in hot toluene. Table 1 summarizes this study and shows that the crosslinking density of EVA network decreases during hydrolysis–condensation reactions all the more the crosslinking density is weak after the first step of crosslinking (value for $t = 0$). Indeed, in the case of VA/OR = 0.5, μ decreases from about 3.6×10^{-4} mol ml^{-1} down to 2×10^{-4} mol ml^{-1} that corresponds to a decrease of about 36% in 4 days, whereas in the case of VA/OR = 2, μ decreases from about 1.4×10^{-4} to 5×10^{-5} mol ml^{-1} (64% in 4 days).

The influence of the initial crosslinking density on the decrosslinking reaction during the step of hydrolysis–condensation can have many explanations. The first one is based upon the well-known sensitivity of alkoxysilane to hydrolysis with respect to the length of alkyl groups [27], weakest sensitivity being observed for the longest alkyl

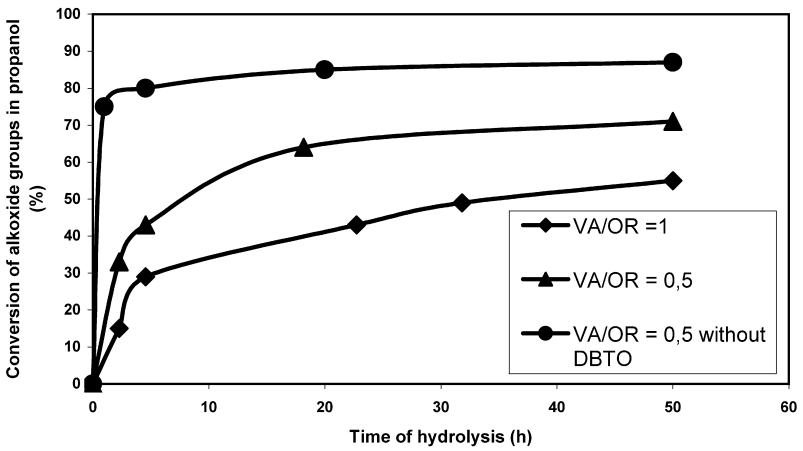

Fig. 4. Variation of propanol versus time of hydrolysis–condensation.

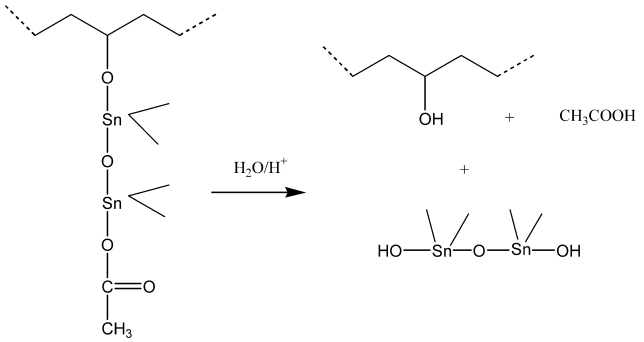

Fig. 5. Reaction scheme of hydrolysis of pendant ester groups of EVA in presence of DBTO.

group. In the present work, each crosslinking bridge is surrounded by 4 segments of about 20 methylene groups which restrict the access of water around Si–O–C bonds through their hydrophobic character. The second one is based on the water diffusion through the organic network which is all the more slowing down than the crosslinking density is higher after the step of crosslinking and before hydrolysis. This decrosslinking reaction constitutes a side–reaction that leads to the formation of silanols at the surface of silica and of alcohol groups on the EVA backbone (Fig. 6). The silanol groups can give hydrogen bonds with pendant ester groups of EVA and contribute to a physical crosslinking. The addition of a powerful hydrogen donor such as hexafluoropropanol in hot toluene after hydrolysis–condensation does not prevent the appearance of a gel phase that confirms the crosslinking of EVA through Si–O–C bonds after hydrolysis–condensation and the hybrid character of the material.

3.4. Evolution of hydrolysis–condensation reactions by MIR spectroscopy

FT-IR spectra were recorded from 400 to 4000 cm^{-1}. Figs. 7 and 8 show the respective evolution of MIR absorbance related to carbonyl bonds (1600–1850 cm^{-1}) and to Si–O–C bonds (900–1300 cm^{-1}) versus time of hydrolysis for samples elaborated with VA/OR = 0.5.

3.4.1. 1600–1800 cm^{-1}

The EVA spectrum shows one main absorbance band around 1740 cm^{-1} associated with carbonyl group of ester

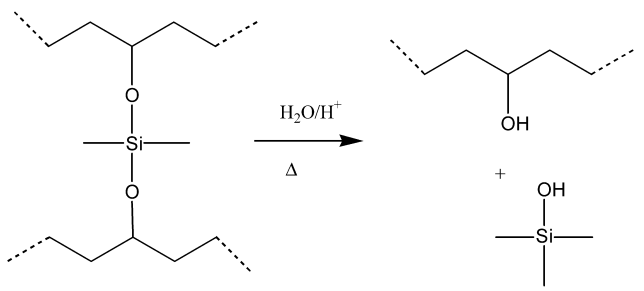

Fig. 6. Reaction scheme of hydrolysis of SiOC bonds linked to the polymer.

Table 1
Variation of the crosslinking density μ (10^4 mol ml^{-1}) versus time of hydrolysis for VA/OR = 0.5, 1 and 2

Time of hydrolysis (days)	0	2	4
VA/OR = 0.5	3.6	2.7	2.3
VA/OR = 1	3.2	2.0	–
VA/OR = 2	1.4	1.1	0.5

and a weak absorbance band around 1700 cm^{-1}. The absorbance associated with the ester group is always present whatever the time of hydrolysis–condensation reactions is. Additionally, during hydrolysis of crosslinked EVA, an absorbance band appears around 1710 cm^{-1} and its intensity increases with the time of hydrolysis. Landry and Coltrain [6] already pointed out this phenomenon in the case of polyvinyl acetate/tetraethoxysilane(TEOS) hybrid elaboration. They associated this absorbance to hydrogen bonds between carbonyl group from polymer and residual silanols after hydrolysis of the tetraethoxysilane (TEOS). In the synthesis of hybrid based upon poly(2-methyl-2-oxazoline), poly(*N*,*N*-dimethylacrylamide) and poly(*N*-vinyl-2-pyrrolidone)/TEOS blends, Saegusa and Chujo [8] also interpreted a shift of carbonyl bands absorbance during hydrolysis–condensation of TEOS as the formation of hydrogen bonds between carbonyl groups and residual silanols of the silica network. However, in the present case this band can have also another origin such as hydrogen bonds between remaining ester groups after the crosslinking and hydrolysis steps and alcohol groups due to hydrolysis of some

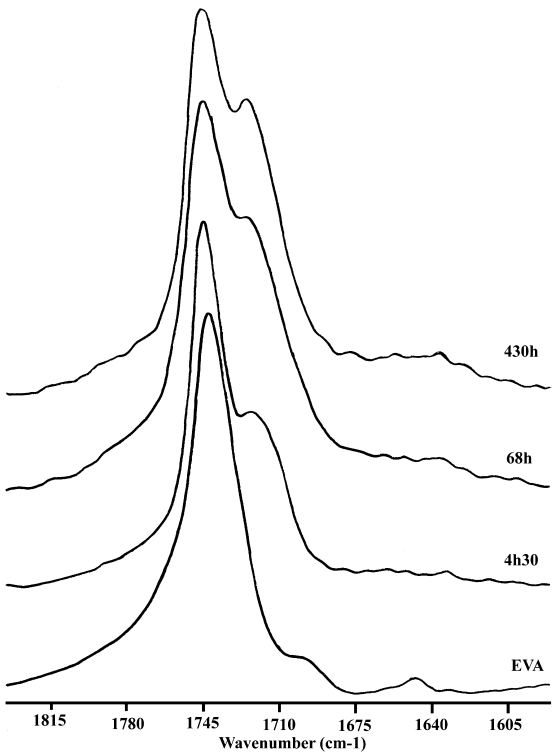

Fig. 7. 1600–1850 cm^{-1} MIR spectra versus time of hydrolysis.

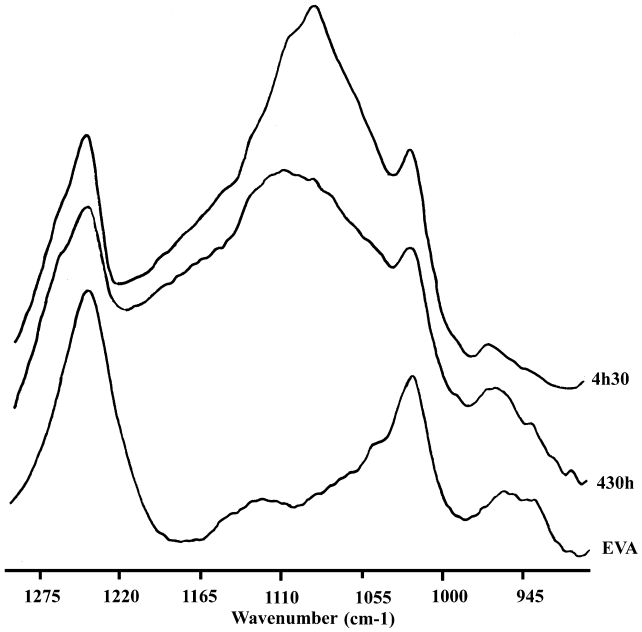

Fig. 8. 900–1300 cm^{-1} MIR spectra versus time of hydrolysis.

crosslinking bridges and grafted distannoxane structure as shown previously.

3.4.2. 900–1300 cm^{-1}

The main modification of the IR spectra in the region 900–1300 cm^{-1}, as the hydrolysis–condensation progresses is the appearance of a peak at 1100 cm^{-1} due to Si–O–Si absorbance as the silica network grows. Parallel to the enlargement of the peak at 1110 cm^{-1}, there is a decrease of the intensity of the band at 1095 cm^{-1} associated with SiOC bonds. Different authors already observed these evolutions during the polymerization in situ of TEOS [5].

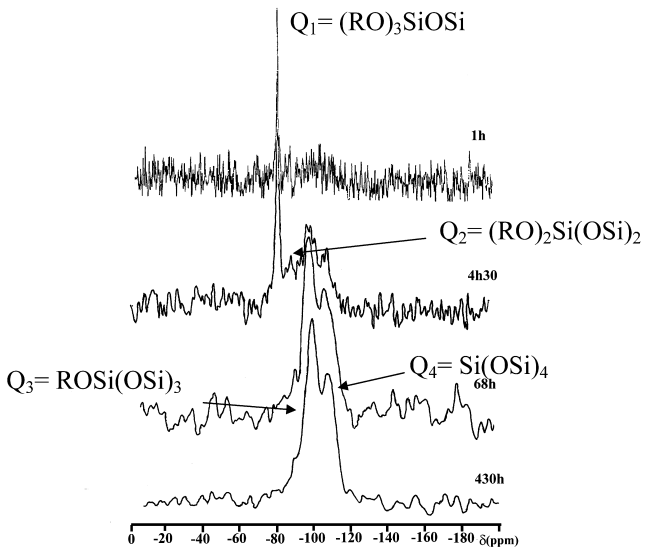

Fig. 9. ^{29}Si solid spectra versus time of hydrolysis.

Table 2
Indexation of ^{29}Si solid NMR peaks

Specie	Formula	δ (ppm)
Q^1	$(RO)_3SiOSi$	−81
Q^2	$(RO)_2Si(OSi)_2$	−92
Q^3	$ROSi(OSi)_3$	−103
Q^4	$Si(OSi)_4$	−112

3.5. Evolution of hydrolysis–condensation reactions by ^{29}Si solid NMR spectroscopy

^{29}Si solid NMR allows following the evolution of silanol condensation (reactions 2 and 3, Fig. 2) leading to SiOSi bonds and to inorganic network during hydrolysis (Fig. 9). The chemical shifts are function of the degree of silanols condensation [28,29] (Table 2). At the beginning of hydrolysis (1 h), only Q^1 species are observed in the background noise. Silanol groups are formed and their condensation has started. After 4 h 30 min of hydrolysis, the intensity of Q^1 increases and three new peaks appear corresponding to Q^2, Q^3 and Q^4 structures that proves that the condensation progresses. The Q^4 structure is characteristic of the silica network formation. As the hydrolysis progresses (68 h), the Q^3 and Q^4 species are accumulated and the silica network becomes denser. Nevertheless, the presence of Q^2 and Q^3 species indicates that the condensation of silanol is not complete in this range of time at 80 °C. Beyond 68 h and until 430 h the respective preponderance of Q^3 and Q^4 species does not change and the condensation does not seem to progress. In addition, these observations are in good agreement with those noticed for example by Landry and Coltrain [6]. Indeed, they observed as in our case, a slight preponderance of Q^3 over Q^4 groups for the acid catalyzed material. On the contrary, base catalyzed gels contain a larger proportion of Q^4 species. However, silanol and alkoxysilane cannot be differentiated with this technique. Consequently, the persistence of the R–O–Si–$(OSi)_3$– structure after 430 h is compatible with SiOC bonds linked to the polymer but also with residual silanol and alkoxysilane grafted onto silica network. These observations are coherent with the previous MIR study.

All the studies used to quantify the hydrolysis–condensation reactions of crosslinked EVA leading to organic–inorganic material conclude that the hydrolysis–condensation of alkoxysilane is not complete. Furthermore the silica network is covalently linked to EVA network and contains non-hydrolyzed propoxide groups. Two side reactions have been elucidated leading to alcohol groups grafted onto EVA backbone. The first one concerns the formation of alcohol groups through hydrolysis of acyloxy-alkoxy distannoxane grafted onto EVA chain. The second one concerns the partial hydrolysis of crosslinking bridges of EVA matrix.

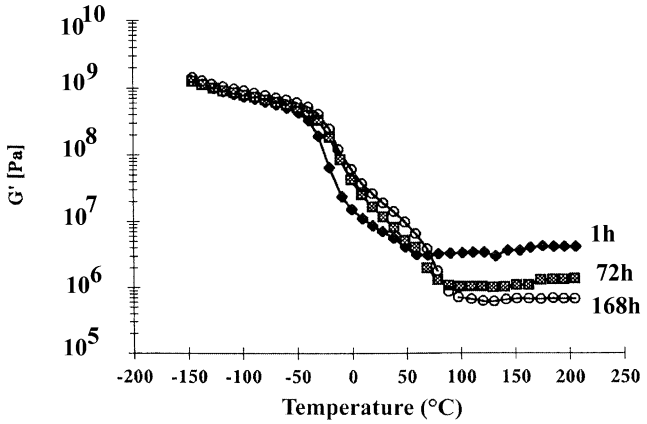

Fig. 10. Variation of storage modulus G' versus temperature for organic–inorganic hybrid after 1, 72 and 168 h of hydrolysis. VA/OR = 0.5, $\omega = 1$ rad s^{-1}.

3.6. Evolution of dynamical thermomechanical properties during hydrolysis–condensation reactions

Figs. 10 and 11 show, respectively, the evolution of storage modulus and the evolution of tg δ versus temperature and time of hydrolysis.

The curves (Fig. 10) show that the crosslinking reactions has drastically changed the viscoelastic properties of EVA at temperature above the melting temperature of crystallites (75 °C) from which a permanent elasticity of the EVA network is observed up to around 200 °C whatever the time of hydrolysis is. However, as hydrolysis progresses, the equilibrium rubber plateau slightly decreases toward a value of about 10^6 Pa. This result is in good agreement with the previous data which showed that the crosslinking density decreases of about 36% with the time of hydrolysis.

Fig. 11 puts in evidence two main transitions for hybrid material after 168 h of hydrolysis condensation at 80 °C. The first one near 0 °C belongs to EVA phase and corresponds to the α transition associated to its glass transition temperature (T_g). T_α is chosen as the maximum of tg δ curves. As shown in Table 3, T_α increases with the time of hydrolysis–condensation and remains constant beyond 168 h. Before hydrolysis, the T_α transition is at −40 °C whereas it is −27 °C for pure EVA. This apparent contradiction is explained by the presence of free TPOS after crosslinking (about 90%) which plasticizes the EVA network although the molecular weight between crosslinking bridges is lower (1750 g mol^{-1}) than the molecular weight between entanglements (about 6000 g mol^{-1}) for EVA used in this study [21,22].

Table 3
Crosslinking density μ (10^4 mol l^{-1}) and T_α (°C) transition of EVA organic–inorganic hybrids at different times of hydrolysis and condensation

Time of hydrolysis (days)	0	2	4	7	18	30
μ	3.2	2.7	2.3	2.2	2.0	2.0
T_α	−40	−18	−10	−4	−2	−2

As the hydrolysis condensation progresses free TPOS is converted in silica. As a first consequence its plasticizer power disappears. Furthermore, as hydrolysis progresses, silica domains are generated and grafted onto polymer network leading to organic and inorganic interpenetrated networks. As a consequence the motions of EVA segments are hindered and T_α transition increases. Besides residual silanols of the silica domains and alcohol groups grafted onto EVA chains through the previous side reactions can also contribute to the increase of T_α.

The curve obtained after 168 h of hydrolysis (Fig. 11) exhibits also a second transition around 90 °C. Its origin is not yet elucidated and will be the aim of a future work. It can be associated with the EVA segments entrapped in the growing silica network during the step of hydrolysis according to the chemical scheme on Fig. 3. Then it would reflect the glass transition of EVA segments linked to the silica network as shown in Fig. 3 and as suggested by other authors for polypropylene oxide/silica hybrid [1]. But because EVA used in this study has a melting temperature at 75 °C this transition might correspond to a contribution of the melting of the crystallites.

3.7. Mechanical properties: tensile strength properties

The mechanical properties of the pure EVA, crosslinked

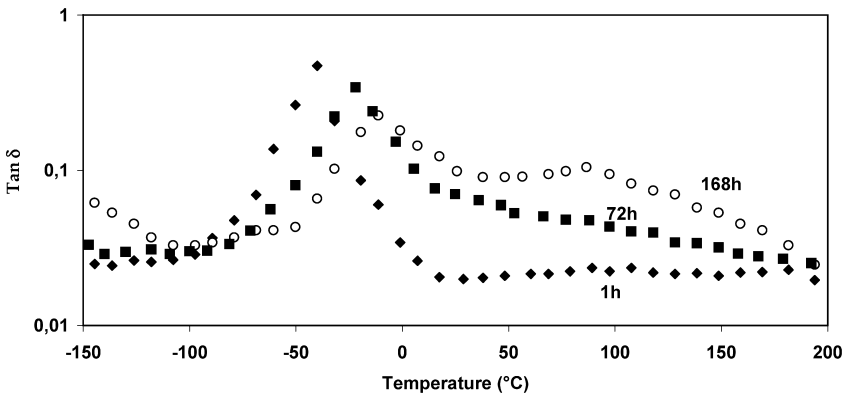

Fig. 11. Variation of tan δ versus temperature for organic–inorganic hybrid after 1, 72 and 168 h of hydrolysis. VA/OR = 0.5, $\omega = 1$ rad s^{-1}.

Table 4
Tensile strength properties of pure EVA, crosslinked EVA and organic–inorganic hybrid (time of hydrolysis: 168 h, VA/OR = 0.5), $T = 25$ °C

	μ (10^4 mol ml^{-1})	Young modulus (MPa)	σ_{break} (MPa)	ε_{break} (%)
EVA	–	30	28	800
Crosslinked EVA	3.0	9	2	25
Organic–inorganic hybrid	2.2	100	22	330

EVA and organic–inorganic hybrid network elaborated with VA/OR = 0.5 and 168 h of hydrolysis are reported in Table 4. As expected, the organic network resulting from the crosslinking reaction between ester and alkoxysilane groups presents brittle properties compared with the pure EVA because the molecular weight between crosslinking bridges (about 1750 g mol^{-1}) is lower than the molecular weight between entanglements (about 6000 g mol^{-1} for EVA uncrosslinked). Indeed, a drastically change of the properties can be observed as the tensile stress and elongation at break drop to, respectively, 2 MPa and 25%. Furthermore, the Young modulus also considerably decreases, and varies from 30 MPa for the pure EVA to 9 MPa for the EVA crosslinked in the presence of TPOS. This drop in magnitude of the Young modulus at room temperature can be explained by the fact that the crystallinity of the EVA decreases with increasing the organic network density as already pointed out in a previous paper [30].

However, after hydrolysis, hybrid material exhibits interesting mechanical properties with a restoration of the elasticity. The material becomes ductile with an elongation at break of about 300% and present an elastomeric behavior. Furthermore, an increase of the Young modulus to 100 MPa can be also reached. These properties of reinforcement can be explained by the presence of silica domains interpenetrated with EVA matrix as previously discussed and illustrated in Fig. 3. Nevertheless, as previously shown by dynamic thermomechanical analysis, the α transition temperature (Table 3) is near 0 °C and it may have an influence on the mechanical behavior investigated at room temperature and more specifically on the increase of the Young modulus.

4. Conclusion

This study showed that it is possible to elaborate an organic–inorganic hybrid material through a melt process without solvent. This synthesis is based upon two successive steps of chemical reactions. The first one consists in an interchange reaction between pendant ester groups from EVA and alkoxide groups from TPOS leading to the EVA network with crosslinking bridges having alkoxysilane groups sensitive to hydrolysis. The second one is based on the hydrolysis–condensation reactions of propoxysilane of crosslinking bridges and free tetrapropoxysilane confined in the polymer network. Gas chromatography, FT-IR spectroscopy, ^{29}Si solid NMR, volume swelling rate at equilibrium in hot toluene and dynamic mechanical analysis showed that the silica network is covalently linked to the polymer network leading to an organic–inorganic hybrid. However, two side reactions have been elucidated during the hydrolysis step leading to alcohol groups on polymer backbone and silanol on silica. These alcohol and silanol groups may contribute to establish hydrogen bonds between SiO_2 domains and acetate groups of EVA chains. These hybrid materials exhibit transparency and improved mechanical properties, especially tensile strength properties with reinforcement due to the in situ synthesis of silica domains but also having an elongation at break of about 300% with an elastomeric behavior. Hence these hybrid materials present a thermomechanical behavior enhanced with respect to the EVA, without flowing beyond the melting temperature of crystallites until 200 °C. Works are in progress to elaborate these hybrid materials by a continuous process such as extrusion.

Acknowledgements

The authors wish to thank Dr Christophe Viton from the same laboratory for the time dedicated to HPLC analysis.

References

[1] Yano S, Iwata K, Kurita K. Mater Sci Engng 1998;C6:75–90.
[2] Huang HH, Orler B, Wilkes GL. Macromolecules 1987;20:1322–30.
[3] Hsu YG, Lin FJ. J Appl Polym Sci 2000;75:275–83.
[4] Girard-Reydet E, Lam TM, Pascault JP. Macromol Chem Phys 1994; 195:149–58.
[5] Landry CJT, Coltrain BK, Wesson JA, Zumbulyadis N, Lippert JL. Polymer 1992;33(7):1496–506.
[6] Landry CJT, Coltrain BK, Landry MR, Fitzgerald JJ, Long VK. Macromolecules 1993;26:3702–12.
[7] Landry CJT, Coltrain BK, Brady BK. Polymer 1992;33(7):1486–95.
[8] Saegusa T, Chujo Y. Makromol Chem, Macromol Symp 1991;51: 1–10.
[9] Huang HH, Wilkes GL, Carlson JG. Polymer 1989;30(11):2001–12.
[10] Noell JLW, Wilkes GL, Mohanty DK, McGrath JE. J Appl Polym Sci 1990;40:1177.
[11] Yano S, Nakamura K, Yamauchi N. J Appl Polym Sci 1994;54: 163–76.
[12] Yano S, Furukawa T, Kodomari M. J Nat Inst Mater Chem Res 1996; 4:231.
[13] Philipp G, Schmidt H. J Non-Cryst Solids 1984;63:283–92.
[14] Jang J, Park H. J Appl Polym Sci 2002;85:2074–83.

[15] Garrido L, Mark JE, Sun CC, Ackerman JL, Chang C. Macromolecules 1991;24:4067–72.
[16] Ikeda Y, Kohjiya S. Polymer 1997;38(17):4417–23.
[17] Start PR, Mauritz KA. J Polym Sci Part B: Polym Phys 2003;41:1563–71.
[18] Wu CS, Liao HT. J Appl Polym Sci 2003;88:966–72.
[19] Bounor-Legaré V, Ferreira I, Verbois A, Cassagnau Ph, Michel A. Polymer 2002;43:6085–92.
[20] French Patent Dow Corning n° 69.43.985; 1968.
[21] Cassagnau P, Bert M, Verney V, Michel A. Polymer 1993;34(1):124–31.
[22] Espinasse I, Cassagnau P, Bert M, Michel A. J Appl Polym Sci 1994;54:2083–9.
[23] Bonetti J, Gondard C, Petiaud R, Llauro MF, Michel A. J Organomet Chem 1994;481:7–17.
[24] Espinasse I, Petiaud R, Llauro MF, Michel A. Int J Polym Anal Characterization 1995;1:137–57.
[25] Bounor-Legaré V, Llauro MF, Monnet C, Michel A. Polym Int, accepted for publication.
[26] Patel SK, Malone S, Cohen C, Gillmor JR, Colby RH. Macromolecules 1992;25:5241–51.
[27] Chen KC, Tsuchiya T, Mackenzie JD. J Non-Cryst Solids 1986;81:227–37.
[28] Maciel GA, Sindorf DW. J Am Chem Soc 1980;102:7606–7.
[29] Lippmaa E, Magi M, Samoson A, Englehardt G, Grimmer A-R. J Am Chem Soc 1980;102:4889–93.
[30] Viallat A, Cohen-Addad JP, Cassagnau P, Michel A. Polymer 1996;37(4):555–64.